PAPER

Covalent functionalization of SWCNT with combretastatin A4 for cancer therapy

To cite this article: Mohyeddin Assali *et al* 2018 *Nanotechnology* **29** 245101

IOP Publishing Nanotechnology
Nanotechnology 29 (2018) 245101 (10pp) https://doi.org/10.1088/1361-6528/aab9f2

Covalent functionalization of SWCNT with combretastatin A4 for cancer therapy

Mohyeddin Assali[1], Abdel Naser Zaid[1], Naim Kittana[2], Deema Hamad[1] and Johnny Amer[2]

[1] Department of Pharmacy, Faculty of Medicine and Health Sciences, An Najah National University, PO Box 7, Nablus, Palestine[†]
[2] Department of Biomedical Sciences, Faculty of Medicine & Health Sciences, An Najah National University, PO Box 7, Nablus, Palestine

E-mail: m.d.assali@najah.edu

Received 9 January 2018, revised 23 February 2018
Accepted for publication 27 March 2018
Published 16 April 2018

Abstract

Single walled carbon nanotubes (SWCNT) are currently under intensive investigation by many labs all over the world for being promising candidates for cancer chemotherapy delivery. On the other hand, combretastatin A4 (CA4) is an anticancer drug that induces cell apoptosis by inhibiting tubulin polymerization. However, it has the disadvantage of low water solubility and the non-selective targeting. Therefore, we aim to create nano-drug from the functionalization of SWCNT covalently with CA4 through click reaction in the presence of tetraethylene glycol linker in order to improve its dispersibility. Scanning electron microscopy and transmission electron microscopy showed good dispersibility of the functionalized SWCNT with diameters of 5–15 nm. Moreover, thermogravometric analysis showed that the efficiency of SWCNT functionalization was around 45%. The *in vitro* release profile of CA4 at physiological conditions showed that approximately 90% of the loaded drug was released over 50 h. After that MTS test was used to determine the suitable concentration range for the *in vitro* investigation of the SWCNT-CA4. After that the cytotoxic activity of the SWCNT-CA4 was evaluated by flow cytometry using annexin V/propidium iodide (PI) test. In comparison with free CA4, SWCNT-CA4 treatment demonstrated a significant increase in necrotic cells (around 50%) at the expense of the proportion of the apoptotic cells. Moreover, cell cycle PI test demonstrated that free CA4 and SWCNT-CA4 caused G2/M arrest. However with CA4 treatment higher proportion of cells were in the S-phase while with SWCNT-CA4 treatment greater proportion of cells appeared to be in the G1-phase. Taken together, the provided data suggest that the novel SWCNT-CA4 has a significant anticancer activity that might be superior to that of free CA4.

Keywords: single walled carbon nanotubes, combretastatin A4, covalent functionalization, anticancer activity, cell cycle

(Some figures may appear in colour only in the online journal)

1. Introduction

Single walled carbon nanotubes (SWCNT) are among the allotropic forms of carbon, where single sheet of six-membered rings of carbon atoms (graphene sheet) wrap into single layered wall of cylindrical tubes with a diameter between 0.4 and 3 nm and a length of 0.2–5 μm, so that a length-to-diameter ratio exceeds 1:10 000 [1, 2]. The large surface area of SWCNT allowed researchers to load large numbers of drug molecules on these particles for the aim of modifying the pharmacokinetic/dynamic properties of these drugs [3]. However, the low dispersibility and high toxicity of pristine SWCNT were hampering obstacles for further clinical applications [4]. Recently, it was found that the

[†] Whilst IOP publishing adheres to and respect UN resolutions regarding the designations of territories (available at http://www.un.org/press/en), the policy of IOP publishing is to use the affiliations provided by its authors on published articles.

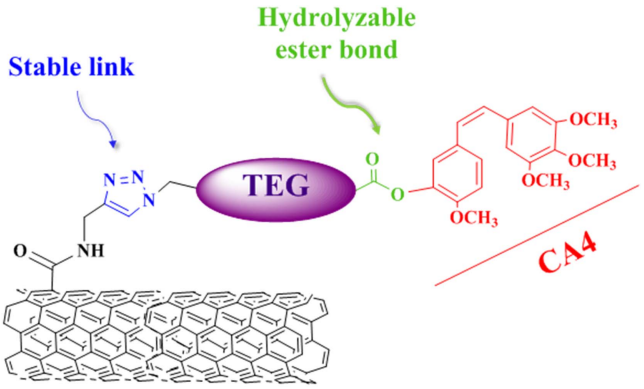

Scheme 1. General scheme of the developed nanosystem.

functionalization of SWCNT with hydrophilic moieties, like branched polyethylene-glycol (PEG) and glucosamine, could significantly decrease their toxicities and improve their water dispersibility by decreasing the reticuloendothelial system uptake and the relatively rapid clearance of the functionalized SWCNT from the organs and excretion from the body. The later advantage would not only be important for drug formulation but also necessary for effective distribution of these macromolecules in different body fluids [5, 6]. This is particularly important especially when loading anticancer drugs on SWCNT, as in this case these macromolecules are expected to distribute from the blood compartment into the tumor tissue compartment more effectively than it would do in the case of distribution into healthy tissues [7–9], which would imply better anticancer drug targeting, greater efficacy and perhaps less side effects. This could be attributed to the fact that the endothelial cells of tumor blood capillaries are normally discontinuous and therefore the cancer blood capillaries could be more permeable to macromolecules as compared to those of normal tissues in a known phenomena called enhanced permeability and retention [10, 11].

Combretastatin A4 (CA4) is a tubulin binding anticancer drug that can effectively depolymerize the microtubules [12, 13] of cancer cells and vascular endothelial cells, resulting cell apoptosis, inhibition of metastasis and suppression of angiogenesis [14–17]. The poor water solubility of CA4 is a major problem. It has been demonstrated that a carrier system like liposomes [18, 19], polymeric nanoparticles and peptide conjugates [20, 21] might improve water solubility, bioavailability and therapeutic efficacy of CA4 [18]. Herein, we aimed to employ a bifuntional tetraethylene glycol (TEG) as a linker to covalently functionalize SWCNT with CA4 through click reaction [22], in a way that an ester bond link CA4 molecules with the complex as shown in scheme 1. We hypothesized that this complex might improve the water solubility of CA4, deliver greater amount of CA4 to the cellular interior, perform as a slow release nano-system and maintain the water dipersibility of SWCNT as TEG moiety attached through a stable link. Therefore, our objective is the covalent functionalization of SWCNT with CA4 in order to improve its anticancer activity.

2. Materials and methods

2.1. Materials

All materials that are used in the experiments were of analytical grade. 2-(3,4,5-trimethoxyphenyl) acetic acid, 3-hydroxy-4-methoxybenzaldehyde, 1-(3-dimethylaminopropyl)-3-ethylcarbodiimide hydrochloride (EDC), L-ascorbic acid sodium salt, propargylamine, quinoline and TEG were purchased from Alfa Aesar Company, England. SWCNT-COOH was brought from carbon solutions, USA. Sodium azide and 1,4-dioxane were purchased from Riedel-de Haën Company, Germany. 4-(dimethylamino) pyridine (DMAP), acetic anhydride, copper, anhydrous copper sulfate and *N*,*N*-diisopropylethylamine (DIPEA) were purchased from Sigma-Aldrich, USA.

All reactions were stirred under ambient conditions. Column chromatography using silica gel (pore size 60 Å, 40–63 μm particle size, 230–400 mesh particle size) purchased from Sigma Aldrich Company was used to purify the products. TLC (DC-Fertigfolien Alugeram®Silg/Uv_{254}, Macherey Nagel Company, Germany) was used to monitor the reactions. Centrifuge (UNIVERSAL 320, Hettich Zentrifugen, Germany) and water path sonicator (MRC DC-200H Digital Ultrasonic Cleaner) were used in preparation and dispersion of functionalized SWCNT.

For cell culture and *in vitro* drug testing, Dulbecco's free Ca^{++}-phosphate buffered saline (PBS), DMEM, L-glutamine solutions, fetal bovine serum (FBS) were purchased from Biological industries, Jerusalem. Trypsin-EDTA solution 1X was purchased from sigma-aldrich, USA. Celltiter 96®Aqueous one solution cell proliferation Assay. Annexin-V-FLUOS-staining Kit was purchased Roche diagnostics, Germany.

2.2. Techniques and equipment

Nuclear magnetic resonance (NMR) spectra were obtained using Bruker Avance 300 spectrometer, Switzerland). Ultraviolet–visible (UV–vis) spectra were recorded with (7315 Spectrophotometer, Jenway, UK), using quartz cuvettes. Thermogravometric analysis spectra were recorded by (STA 409 PC Luxx®, NETZSCH) in 25 °C–600 °C, flow 20 °C under nitrogen (100 cc min^{-1}). Transmission electron microscopy (TEM) images were taken by using Morgagni 286 transmission microscope (FEI Company, Eindhoven, Netherlands) at 60 kV. Scanning electron microscopy (SEM) images were taken by Inspect F50 SEM (FEI Company, Hillsboro, USA) with 1000 000 times magnification. Infrared spectroscopy (IR): Nicolet iS5, ThermoFisher Scientific Company, USA. Flow cytometry: FACS caliber, Becton Dickinson, Immuno-fluorometry systems, Mountain View, CA. High performance liquid chromatography (HPLC) dionex ultimate 3000.

2.3. Synthesis and functionalization of SWCNT

In order to functionalize SWCNT with combrestastatin A4 (CA4), a derivative of TEG was used as a hydrophilic linker

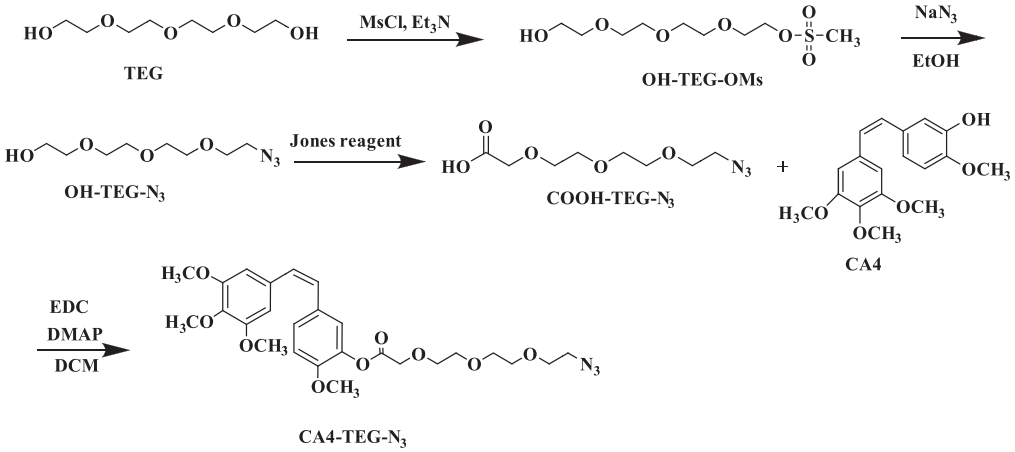

Scheme 2. Synthesis of CA4-TEG-N_3.

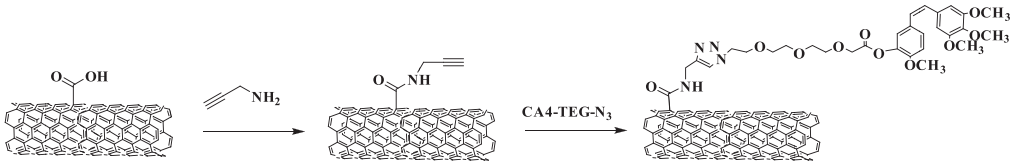

Scheme 3. Functionalization of SWCNT with CA4 through click reaction.

between CA4 and SWCNT. The linker was synthesized using several steps started with the reaction of OH group of TEG with mesyl group to get compound OH-TEG-OMs. After that, the mesyl group was replaced with azide group through the reaction with sodium azide in ethanol to get OH-TEG-N_3. Then, it oxidized using Jones reagent to prepare the required linker COOH-TEG-N_3 followed by esterification reaction with CA4 through using EDC as a coupling agent and DMAP as a catalyst to synthesized CA4-TEG-N_3 as shown in scheme 2.

After the successful synthesis of CA4-TEG-N_3, the carboxylated-SWCNT were functionalized covalently with propargylamine through amidation reaction to get terminal alkyne group. After that, the alkyne-SWCNT were effectively bind with CA4-TEG-N_3 through click reaction, which is occurred in one pot and produced a high yield reaction with a minimum byproduct [22, 23]. It is performed in various copper catalyst, here in we used anhydrous $CuSO_4$ in the presence of ascorbic acid dissolved in a mixture DCM:H_2O to functionalize the SWCNT with CA4 as shown in the scheme 3. Therefore, the direct connection with the SWCNT was through triazole group that are highly enzymatic and chemically stable and the linkage with the CA4 was through an ester bond that can be hydrolyzed by esterase enzyme in order to give a controlled release profile of the anticancer drug. Moreover, after the release of CA4, the SWCNT still will be functionalized with the TEG derivative that ensures its biocompatibility and safety as reported previously [24–26].

2.3.1. Synthesis of COOH-TEG-N_3. It was synthesized according to the disclosed method (scheme 2) [27]. Briefly, to a solution of TEG (10 g, 51.5 mmol) and triethylamine (7 ml, 51.5 mmol) in 50 ml THF stirred for 5 min and cooled at 0 °C, mesyl chloride (4 ml, 51.5 mmol) was added dropwise over a period of 30 min. The reaction was stirred vigorously for 24 h at room temperature. The product was extracted with DCM (250 ml) and washed with HCl 1 M (50 ml) and brine (50 ml). DCM was dried over Na_2SO_4, filtered and evaporated. The product was pale yellow oil purified by flash column chromatography in DCM/MeOH (20:1). To obtain OH-TEG-OMs with a yield of 28%. R_f: 0.5 (DCM/MeOH 9:1).

To a solution of OH-TEG-OMs (1.8 g, 6.62 mmol) dissolved in 10 ml ethanol, sodium azide (516.0 mg, 7.94 mmol) was added. The reaction was stirred at 70 °C overnight. Ethanol was evaporated and the reaction was extracted with 100 ml of diethyl ether and 40 ml of brine. Diethyl ether dried over Na_2SO_4, filtered and evaporated the product was pale yellow oil to obtain OH-TEG-N_3 with a yield of 85%. R_f: 0.39 (DCM/MeOH 20:1).

Finally, Jones reagent (22 ml) was added to a solution of OH-TEG-N_3 (600 mg, 2.7 mmol) dissolved in acetone (22 ml), the reaction was stirred for 2 h. After that, isopropyl alcohol was added to the reaction to quench the excess of Jones reagent. Then, the reaction solution was filtrated using Celite® and washed by DCM, the product was extracted by 40 ml of saturated $NaHCO_3$. The aqueous layer was washed with 100 ml of DCM and acidified with HCl (2 M). DCM was dried over Na_2SO_4, filtrated and evaporated to obtain the desired product COOH-TEG-N_3 with a yield of 95%. R_f: 0.4 (DCM/MeOH 9:1).

The chemical structure of all products were confirmed by HRMS, and ^1H and ^{13}C NMR spectroscopies, which could be found in previous publication [27].

2.3.2. Synthesis of combretastatin (CA-4). The CA4 was synthesized according to the method published by Xiao *et al* with some modification (scheme 3) [28]. Triethylamine (2.22 ml, 15.91 mmol) was added to a solution of (2-(3,4,5-trimethoxyphenyl) acetic acid (3 g, 13.26 mmol), 3-hydroxy-4-methoxybenzaldehyde (2.421 g, 15.91 mmol) and acetic anhydride (4.38 ml, 46.41 mmol). The reaction was kept at 110 °C for 4 h. After that, the reaction was cooled to room temperature and acidified using 2 M HCl solution. Then, the reaction was stirred in ice bath overnight. The obtained dark yellowish solid was dissolved in 10% NaOH (30 ml), washed and discolored with ethyl acetate (100 ml). HCl 2 M was added until pH (3–4), the precipitated solid was filtrated and recrystallized from EtOAc to give the derivative of acrylic acid.

To derivative of acrylic acid (3.29 g, 9.16 mmol) and copper (4.66 g, 73.26 mmol) dried under vacuum and argon, quinoline (15 ml) was added. The reaction was stirred at 200 °C for 3 h. After that, the reaction was cooled and filtrated. The filtrate was extracted with EtOAc (110 ml) and HCl 2 M (60 ml), the EtOAc layer was washed with saturated NaCl (60 ml) and was dried over Na_2SO_4 to get brown viscous solid which purified by flash column chromatography in n-hexane/ethyl acetate (7:3). The recrystallized was achieved by ethyl acetate: petroleum ether to afford colorless crystals of CA4. Yield 36.4% (1.21 g, 3.8 mmol of product). R_f: 0.23 (Hex/EtOAc 7:3).

^{1}H NMR (300 MHz, $CDCl_3$):δ 6.90 (s, 1H, CH, C10 Ar), 6.77 (d, J = 8.19 Hz, 1H, CH, C11 Ar), 6.71 (d, J = 8.19 Hz, 1H, 1CH, C13 Ar), 6.51(s, 2H, 2CH, Ar), 6.39 (d, J = 12.1 Hz, 1H, CH=CH), 6.45 (d, J = 12.1 Hz, 1H, CH, CH=CH), 5.50 (s, 1H, OH), 3.82–3.84 (s, 6H, $2OCH_3$), 3.68 (s, 6H, $2OCH_3$).

IR: 3439.54, 2935.13, 2838.7, 1734.66, 1685.48, 1579.41, 1506.13 cm^{-1}.

HPLC: The purity of cis-CA4 was 96.4% according to the HPLC measurements. A C-18 column (inertsil® OSD-3V, 4.6 × 250 mm, 5 μm) was used with a mobile phase of 0.1% TFA in H_2O (eluent A) and 0.1%TFA in CH_3CN (eluent B). The eluent gradient was set from 20% to 100% B in 30 min with a flow rate 1 ml min^{-1} and the pressure was 107 bar. The CA4 was detected by measuring absorbance at 295 nm.

2.3.3. Synthesis of CA4-TEG-N_3. A solution of CA4 (200 mg, 0.629 mmol), COOH-TEG-N_3 (221 mg, 0.95 mmol), EDC (182 mg, 0.95 mmol) and 4-(dimethylamino)pyridine (116 mg, 0.95 mmol) in dichloromethane (5 ml) was stirred for 19 h under argon. The reaction was extracted with 40 ml of HCl (1 M) and 120 ml DCM, aqueous layer was washed with DCM (2 × 50 ml), and the organic layer was dried over Na_2SO_4, filtrated and evaporated. The product was purified by silica gel by Hex/EtOAc (1:1). (Yield 69%, 233 mg, 0.44 mmol). R_f: 0.23 (Hex/EtOAc 1:1). ^{1}H NMR (300 MHz, $CDCl_3$): δ 7.06 (d, 2H, 2CH, Ar), 6.95 (d, 1H, CH, Ar), 6.78 (d, J = 8.56 Hz, 2H, 2CH, Ar), 6.39 (d, J = 12.1 Hz, 1H, CH=CH), 6.45 (d, J = 12.1 Hz, 1H, CH, CH=CH), 4.33 (s, 2H, CH_2, $COOCH_2$), 3.95–3.76 (m, 22H, CH_2/CH_3, OCH_2CH_2O/OCH_3), 3.3 (t, 2H, J = 5.87 Hz CH_2, CH_2N_3). ^{13}C NMR (125.7 MHz, $CDCl_3$):δ 50.70, 55.95, 60.90, 68.33, 70.05, 70.66, 70.68, 70.96, 105.90, 112.08, 123.02, 127.90, 128.47, 129.71, 130.20, 132.39, 137.24, 138.96, 150.07, 153.01, 168.46. IR: 2961.16, 2922.59, 2102.03, 1776.12, 1613.16, 1578.45, 1507.1 cm^{-1}.

2.3.4. Functionalization of carboxylated-SWCNT with proprgylamine. To carboxylated SWCNT (75 mg) solubilized in DMF (30 ml). EDC (30 mg, 0.16 mmol) and triethylamine (300 μl, 2.19 mmol) were added. The solution was sonicated for 1 h, then the propargylamine (52 μl, 0.82 mmol) was added. The reaction was sonicated for 10 min and stirred for 72 h. $CHCl_3$ (25 ml) was added to reaction, centrifuged for 10 min at 15 000 rpm, supernatant was discarded. Washing process was repeated with $CHCl_3$ (2 × 20 ml), DCM (10 ml) and diethyl ether (2 × 10 ml). The black powder was dried under vacuum. The obtained weight was 69 mg. IR: 3330 (HC≡C), 2130 (C≡C) cm^{-1}.

2.3.5. Click reaction of the SWCNT-alkyne with CA4-TEG-N_3. To anhydrous copper sulfate (7.9 mg, 0.05 mmol), L-ascorbic acid sodium salt (3 mg, 0.02 mmol) dissolved in 4 ml of distilled H_2O was added, the solution was added to a sonicated solution of CA4-TEG-N_3 (65 mg, 0.11 mmol), and Alkyne-SWCNT (30 mg) dissolved in 4 ml of DCM. The solution was sonicated for 10 min. The reaction was stirred overnight. MeOH (15 ml) was added to reaction, sonicated then centrifuged at 15 000 rpm for 10 min, supernatant was discarded followed by two washing steps with MeOH (2 × 15 ml) and ether (2 × 15 ml), black powder was dried. The obtained weight was 25 mg.

2.4. In vitro drug release

In vitro release study, using dialysis bag diffusion technique in 10% FBS PBS, was conducted on SWCNT-CA4 in order to estimate the kinetic release pattern of the CA4 from SWCNT.

2.4.1. Preparation of PBS. 1.0 l PBS (pH 7.4) was prepared according to the literatures [29, 30].

2.4.2. Calibration curve of CA4. A calibration curve was developed by plotting absorbance versus concentration in order to quantify the amount of loaded CA4 on SWCNT. Accordingly, CA4 stock solution was prepared by dissolving an amount of 1 mg ± 0.1 in 10% FBS diluted with adequate volume of PBS. A series of dilutions (0.02, 0.1, 0.3, 0.5 mg ml^{-1}) were prepared by diluting the required volume of the standard solution in adequate volume of solvent. After UV–vis spectroscopic scanning of the stock solution, the drug showed maximum absorbance at 300 nm (λ_{max}) and therefore it was selected for the assessment of its concentration.

2.4.3. Dialysis membrane method. A weighed amount of SWCNT-CA4 (1 mg ± 0.1) was dispersed in 1 ml of a freshly prepared 10% FBS phosphate buffer solution and

transferred into the dialysis bag (spectra/Por® 4). The filled bag was immersed in 150 ml of the prepare PBS and kept under gentle and continuous stirring for 54 h at 37 °C. An aliquot (1 ml) was withdrawn from the release medium at each specified time periods and was replace with equal volume of fresh medium to mimic the sink condition. The absorbance of the collected samples was measured at 300 nm using UV/vis spectrophotometer.

2.5. Anticancer activity

2.5.1. Cell line. The anticancer activity of SWCNT-CA4 was studied against HeLa cells and it was compared with the activity of the free CA4.

2.5.2. Cell culture. HeLa cells were cultured in 15 cm^2 plastic culture plate in culture growth medium (CGM) which consists of DMEM medium supplemented with 10% FBS, L-glutamine and penicillin/streptomycin. Cells were maintained in the above medium at 37 °C and 5% CO_2 in a humidified atmosphere. For sub-culturing, the CGM was suctioned from 15 cm^2 culture plate. Then, the cells were washed with 15 ml of Ca^{2+}-free PBS. After that, 5 ml of trypsin was added to cells and were incubated for 3 min in a humidified atmosphere containing 5% CO_2 at 37 °C until sufficient cells detachment from the surface of the plates. After that, trypsin was inactivated by 20 ml of CGM, and subsequently the cell suspension was collected, diluted and distributed into either 96-well plate or 12-well.

2.5.3. Cell viability test. HeLa cells cultured 96-well plate were incubated with 100 μl/well CGM supplemented with different concentrations of CA4 and SWCNT-CA4 (15, 30 and 60 ng ml^{-1}) over different time intervals (0, 24, 48 and 72 h). After that, 20 μl of MTS solutions was added to each well followed by an incubation period of 1 h at 37 °C and 5% CO_2, before the absorbance was measured by a plate reader at a wave length of 490 nm.

2.5.4. Flow cytometric analysis. HeLa cells cultured in 12-well plates were treated with different concentrations (5, 10 or 15 ng ml^{-1}) of CA4 and SWCNT-CA4; the cells were incubated with treatment solutions for 48 h. After that, studies on apoptosis/necrosis and cell-cycle were conducted by using a flow cytometer (FACS caliber, Becton Dickinson, Immuno-fluorometry systems, Mountain View, CA) as shown below.

2.5.4.1. Apoptosis and necrosis assay. After 48 h of incubation, both adherent and non-adherent cells were harvested mechanically, washed once with PBS and suspended in 250 μl of Ca^{+2} free PBS. Then the cells were treated with (5 μl/100 μl) of annexin-V and incubated at room temperature for 15 min. After that, cells were washed with PBS and incubated with (5 μl/500 μl) of propidium iodide solution (PI) solution. Finally the stained cell suspension were analyzed by flow cytometery.

2.5.4.2. Cell cycle assay. After 48 h of incubation with the treatment conditions, the adhered and non-adhered cells were harvested mechanically and centrifuged at RCF = 150 g for 10 min. The supernatant was discarded. 1 μl of 70% MeOH was added to the cell pellet and incubated at −20 °C for 20 min to permeabilize the cell membrane. The pellet was then washed once with 1.5 ml of PBS. Then, the pellet was resuspended in PI solution and was incubated for 15 min before being analyzed with flow cytometry. Data analysis was carried out using FCS Express 6 (De novo software).

3. Results and discussion

After the functionalization of SWCNT, the dispersibility of pristine SWCNT and SWCNT-CA4 in water was conducted. The *p*-SWCNT formed a clear black sediment after being suspended in water, while SWCNT-CA4 showed a good water dispersibility as shown in figure 1(I). In fact, the *p*-SWCNT have hydrophobic characteristics, which encourage the rapid reaggregation of these nanotubes. On the other hand, SWCNT-CA4 formed a stable black suspensions due to the increase in the hydrophilicity, which was gained by the new functionalization of SWCNT. The morphology and the size of *p*-SWCNT and SWCNT-CA4 were investigated by TEM and SEM images. In both images the *p*-SWCNT appeared as aggregated nanotubes and aggregated bundles due to the hydrophobic interaction between the tubes as shown in figures 1(II) and (III). On the other hand, the functionalized SWCNT-CA4 appeared as individual separated nanotubes with a diameter in the range of (5–15) nm as measured by TEM. In fact, the chemical functionalization of the SWCNT caused a separation and de-bundling effect due to the decrease in the hydrophobic interaction between the nanotubes side walls as shown in figures 1(IV) and (V).

Once the functionalization has been confirmed, the loaded amount of CA4 was measured by spectrophotometery. A calibration curve of CA4 has been built and the loaded amount of CA4 on SWCNT was determined about 0.223 mg in 1 mg of SWCNT-CA4.

Moreover, the percentage of functionalization was confirmed by thermogravimetric analysis. Upon the heating of the functionalized SWCNT (SWCNT-CA4) to 600 °C, the weight loss will be related to the percentage of functionalization as the SWCNT are considered thermo stable [31]. Therefore, a 45% of weight loss was observed which referred to the percentage of functionalization as show in figure 2. Taking into the account the molecular weight ratio of CA4 to the whole conjugate (∼1:2), the percentage of the loaded CA4 would be 23% w/w which coincide with the spectrophotometeric results.

In order to determine that CA4 can be released from the SWCNT in a controlled manner, an *in vitro* release profile was conducted. A time dependent cumulative release of CA4

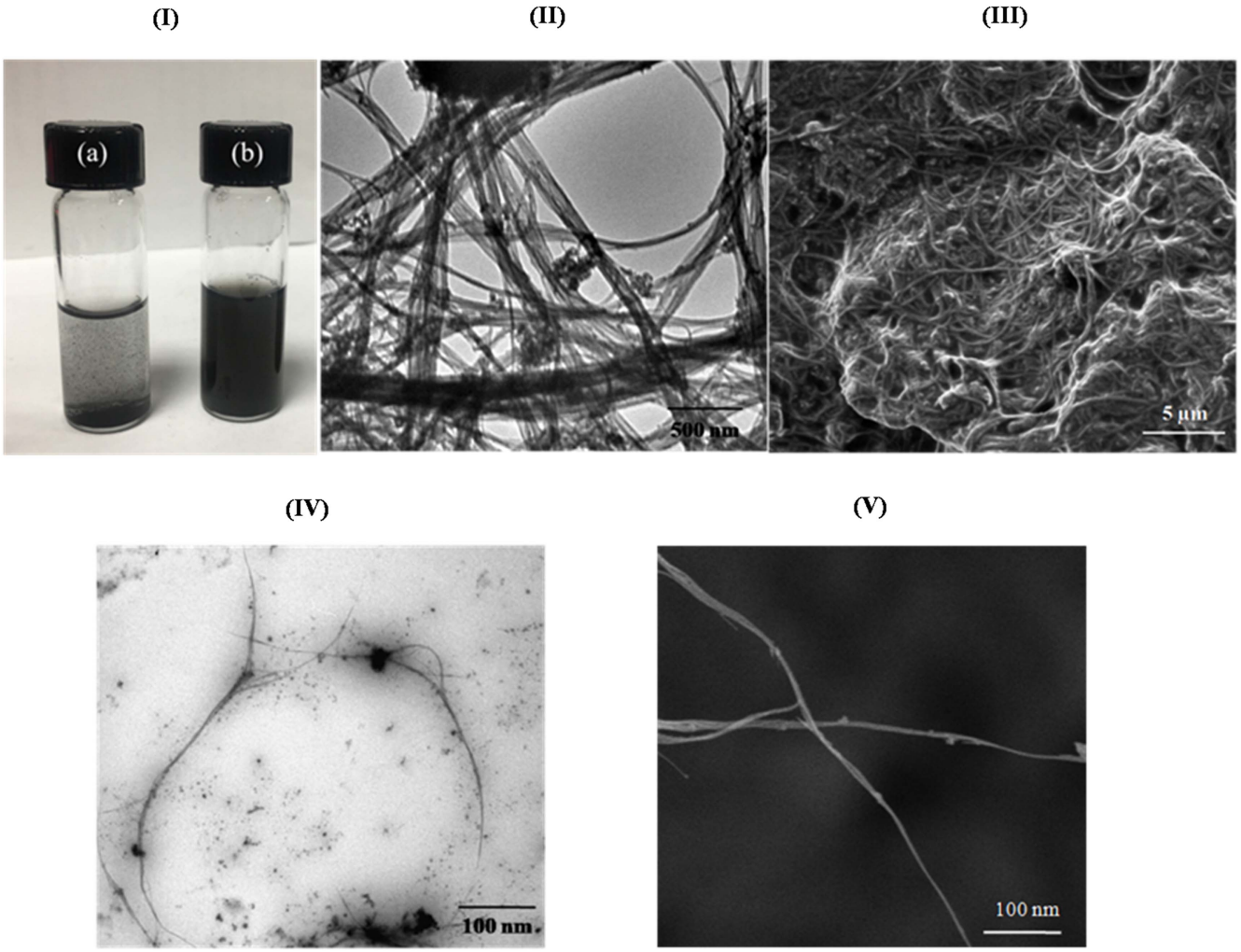

Figure 1. (I) Photograph of dispersions of (a) *p*-SWCNT, and (b) SWCNT-CA4; (II) TEM image of *p*-SWCNT; (III) SEM image of *p*-SWCNT; (IV) TEM image of SWCNT-CA4; (V) SEM image of SWCNT-CA4.

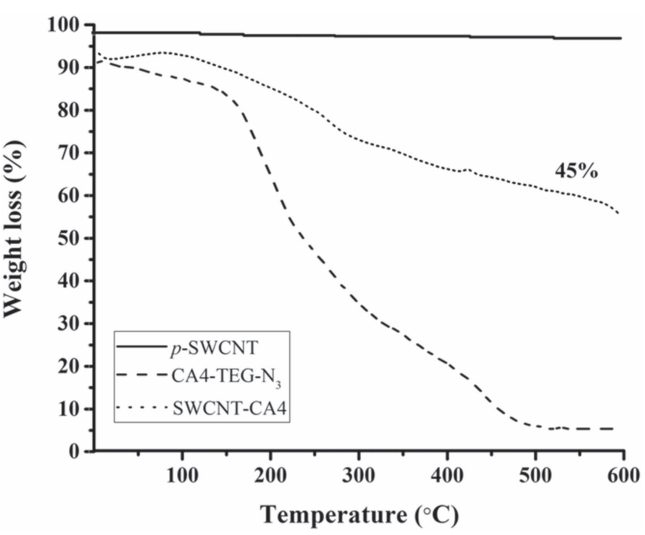

Figure 2. TGA spectra of pristine SWCNT (solid line), SWCNT-CA4 (dot line) and CA4-TEG-N_3 (dash line).

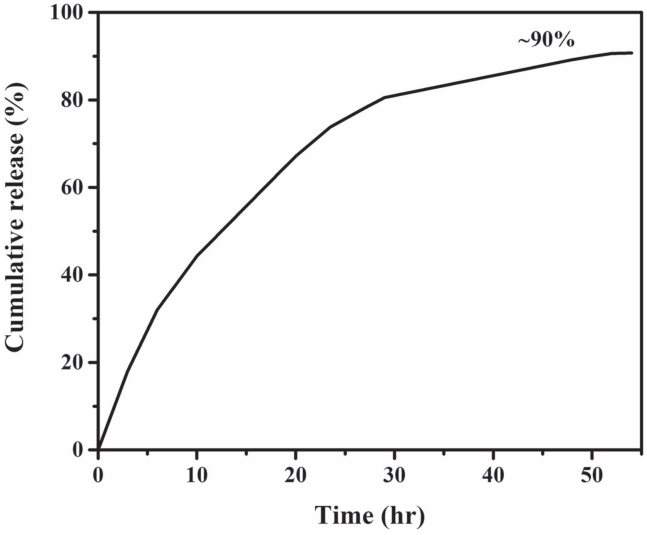

Figure 3. *In vitro* release profile of CA4 from SWCNT-CA4 in phosphate buffer (10% FBS) solution kept at pH 7.4 at 37 °C.

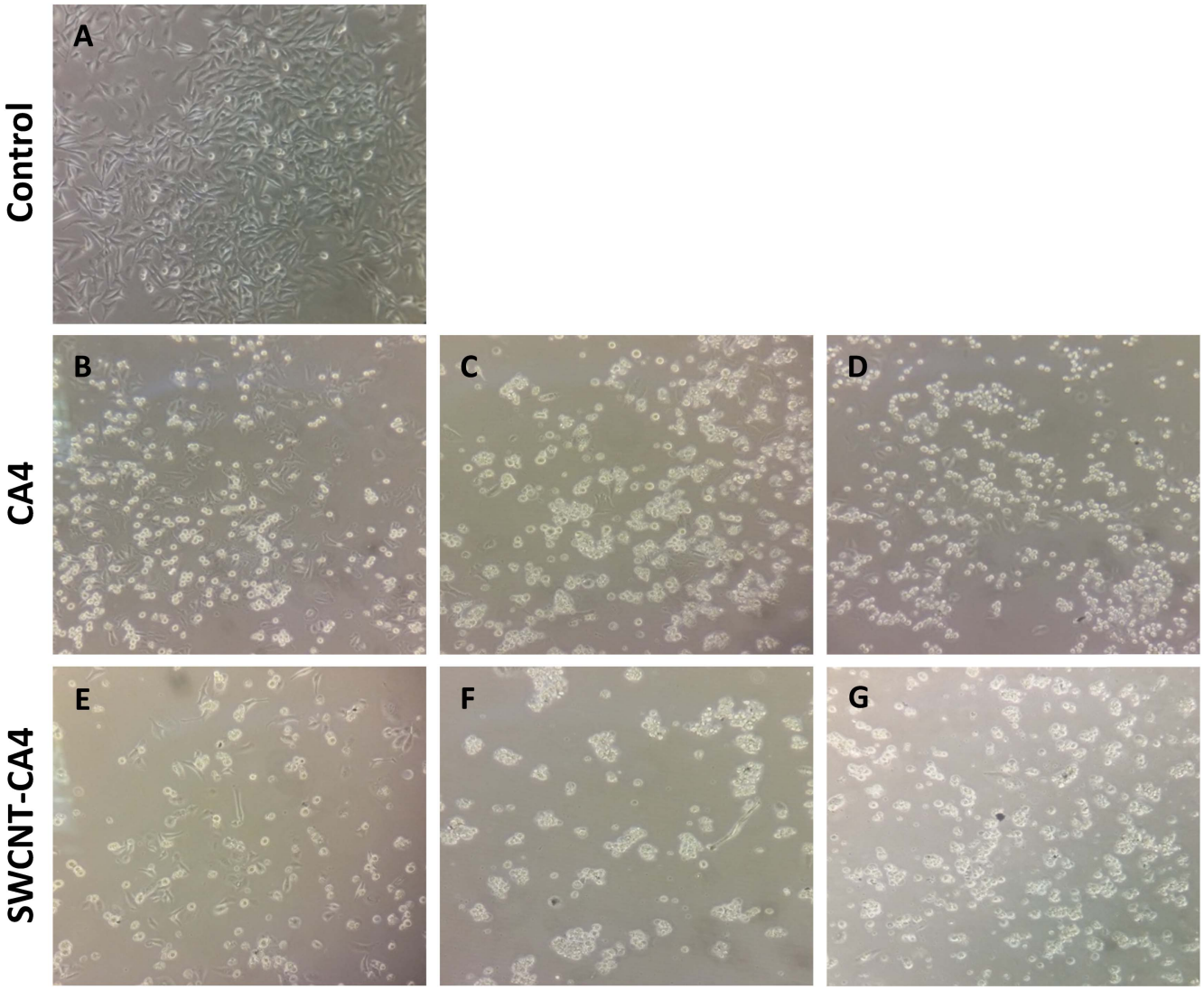

Figure 4. Bright field images at 100× for HeLa cells treated with different concentrations of CA4 (15, 30 and 60) ng ml^{-1}, images (B)–(D), respectively) and different concentrations of SWCNT-CA4 (15, 30 and 60 ng ml^{-1}, images (E)–(G), respectively). Control cells (image (A)) received no treatment.

from SWCNT-CA4 was conducted in 10% FBS-phosphate buffer at pH 7.4 and kept at 37 °C using a dialysis technique. As shown in figure 3, about 32% of the loaded CA4 was released over the first 6 h. After 24 h 74% was released and by the 50th h around 90% of the loaded CA4 had already been released. These results provide an evidence for a controlled release manner for the loaded CA4 by slow ester bond hydrolysis.

The anticancer activity of SWCNT-CA4 was investigated on HeLa cells. Initially, it was necessary to determine the suitable concentration of the test drug and the proper incubation time, therefore as a starting point the effect of different concentration 15, 30 and 60 ng ml^{-1} of both SWCNT-CA4 and free CA4 was investigated on the morphology of HeLa cells at different time intervals; 6, 24 and 48 h (where concentration less than 15 ng ml^{-1} did not show any effect—data not shown—). After 6 h none of the treatment conditions produced any notable morphological changes (images not shown). After 24 h, the 60 ng ml^{-1} of CA4 caused rounding up and detachment of most HeLa cells, while only a few cells detached by the other concentrations of CA4 and SWCNT-CA4 (images not shown). By looking at the cells treated with CA4 (figures 4(B)–(D)) over 48 h, the majority of the cells rounded up and detached by the 30 ng ml^{-1}, while almost half of the cells detached by the 15 ng ml^{-1}. Interestingly, SWCNT-CA4 started producing an effect only after 48 h, when the majority of the cells rounded up and detached by the 60 and 30 ng ml^{-1} (figures 4(F) and (G), while by the 15 ng ml^{-1} roughly 70% of the cells detached (figure 4(E)).

Since cell detachment does not necessarily imply cell death, the MTS proliferation assay was implemented in order to objectively estimate the cell viability under the aforementioned concentrations of SWCNT-CA4 over 48 h treatment interval, which was the minimal time period required for the drug to affect the cells as demonstrated in the previous experiment. The results showed that at a concentration of 15 ng ml^{-1}, the absorbance ratio declined by 65%, while it declined by almost 80% at the concentrations 30 and

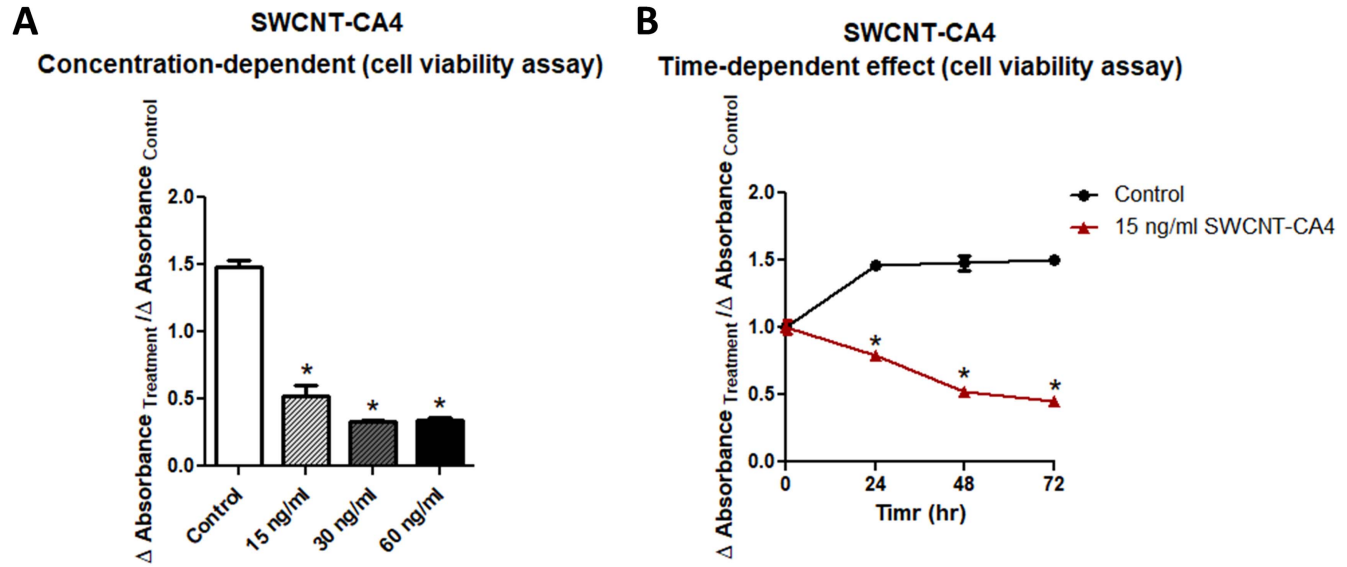

Figure 5. Results for MTS test for indirect estimation of cell viability. (A) Concentration-dependent effect for SWCNT-CA4 on the viability of HeLa cells over 48 h. Student t-test was applied to compare the means, $n = 3$, * $p \leqslant 0.05$ compared to control. (B) The time-dependent effect for the 15 ng ml^{-1} of SWCNT-CA4 on the viability of HeLa cells. $n = 3$, * $p \leqslant 0.05$ compared to control.

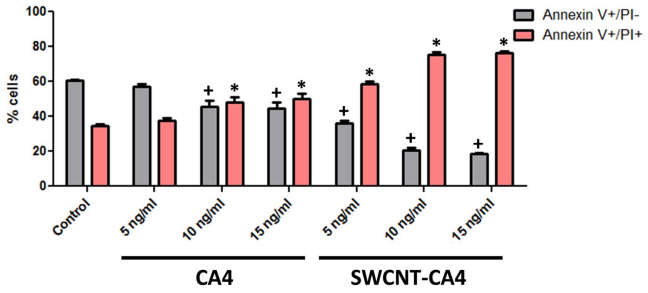

Figure 6. The annexin V/PI test for investigating the effect of different concentrations of CA4 and SWCNT-CA4 on cell necrosis and apoptosis after 48 h incubation. Student t-test was applied to compare the means. $+P$ value $\leqslant 0.05$ compared to control annexin V $+$/PI–, $^{*}P$ value $\leqslant 0.05$ compared to control annexin V+/PI+.

60 ng ml^{-1} (figure 5). This data is coherent with the microscopic images shown before for the same treatment conditions (figure 4). However, due to this high cytotoxicity, it was not possible to implement these two concentrations for the subsequent annexin V/PI flow cytometric analysis, since the cells could not retain the fluorescent dye, which might be due to a severe damage in the membranes of the dead cells. Therefore it was decided to focus on the 15 ng ml^{-1} concentration. For this concentration a time-dependent effect was investigated over treatment intervals of 24, 48 and 72 h. After 24 h, the absorbance ratio increased by around 50%, while it declined by around 25% for the cells treated with SWCNT-CA4 which could be due to cell proliferation in the absence of a cytotoxic action for the drug at this time point. This result is in accordance with the microscopic images shown in figure 4. Interestingly, the absorbance ratio started to decline over 48 and 72 h, which is also in agreement with the images in figure 4. By taking these findings together with the *in vitro* release profile of CA4 from SWCNT-CA4 (figure 3), where a 90% release of CA4 could be achieved over 50 h, it can be assumed that SWCNT-CA4 might be acting as a nano-slow drug release system.

In order to gain a deeper insight to the effect of SWCNT-CA4 on cell viability by determining the percentages of the necrotic and apoptotic cells, the HeLa cells were incubated over 48 h with three concentrations (15, 10 and 5 ng ml^{-1}) of SWCNT-CA4 or CA4, after that they were stained with the annexin V and PI fluorescent dyes, subsequently the cells were analyzed by flow cytometry.

PI is a red fluorescent stain that binds specifically to DNA, however because of its physicochemical properties it cannot permeate through the cell membrane or the nuclear envelope unless the cell is damaged by necrosis or is in late stages of apoptosis, when the permeability of the cellular membranes is severely disrupted. Therefore, by using PI stain alone the necrotic cells and those in late stages of apoptosis specifically fluoresce red color.

On the other hand annexin-V is a green fluorescent dye that specifically binds to phosphatidylserine, which translocates to the exterior surface of the cell membrane starting from the early stages of apoptosis. Therefore, these cells specifically fluoresce green color. PI cannot satin these cells at this stage as the membrane permeability is not sufficient, however when the cells reach late stages of apoptosis or become necrotic then they can be stained by both PI and annexin V [32, 33]. Therefore and in comparison with the free CA4, the treatment with SWCNT-CA4 demonstrated a significant increase in necrotic cells (around 50%) at the expense of the proportion of the apoptotic cells (figure 6).

Moreover, the cell cycle specificity was investigated by using PI test. The data shown in figure 7 demonstrated that free CA4 (15 ng ml^{-1}) and SWCNT-CA4 (15 ng ml^{-1}) caused G2/M arrest, while with CA4 treatment higher proportion of cells were in the S-phase while greater proportion of cells appeared to be in the G1-phase after treatment with SWCNT-CA4. However,

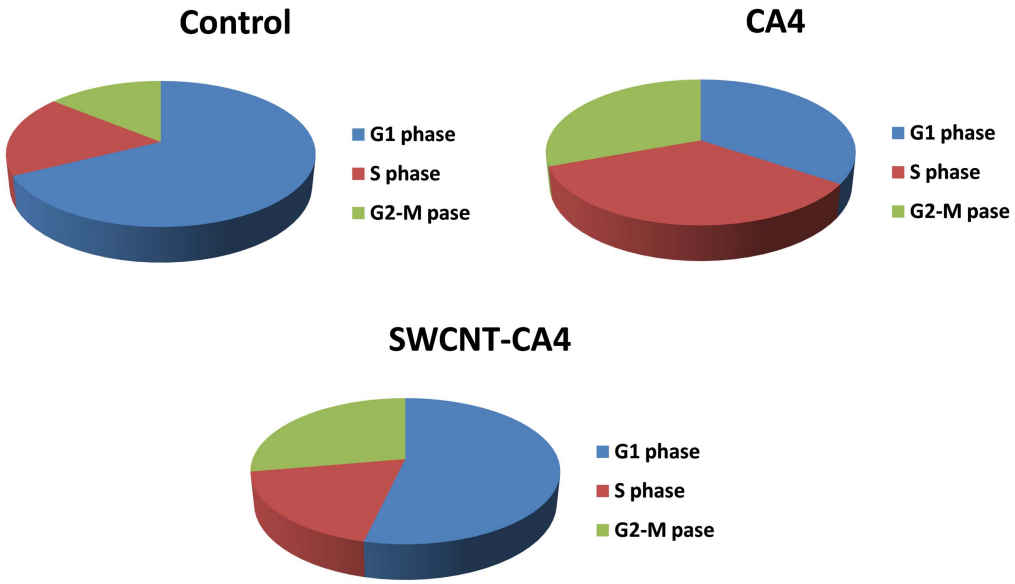

Figure 7. The cell cycle specificity for CA4 and SWCNT-CA4. The pie charts demonstrates the proportion of cells at each phase of the cell cycle.

it is believed that this might not necessarily imply that more cells were actually arrested in that phase. This assumption is based on the fact that the principle of this flow cytometry assay is based on the ability of the PI stain to bind DNA in the nuclei. The more the cells have DNA the higher are the amount of the bound PI and consequently the stronger would be the signal detected by the flow cytometer. Apparently the cells treated with SWCNT-CA4 were harmed by the treatment and the nuclei might have become more leaky, and therefore more DNA might have been lost during the washing step, which might have consequently shifted the signal form the region of S-phase to the region of G1 phase where it might have overlapped with the signal of the cells that are actually in G1-phase [34].

4. Conclusions

The covalent functionalization of SWCNT with CA4 was achieved successfully. The water dispersibility was improved and confirmed by TEM and SEM images. Moreover, CA4 was released from SWCNT-CA4 in a sustained-release manner over 50 h at physiological conditions. More interestingly, the anticancer activity of SWCNT-CA4 was improved in comparison with the free CA4 as shown by the MTS test and annexin V/PI assay. The developed SWCNT-CA4 nanosystem might have the potential to improve the anticancer activity of CA4 and could provide a novel therapy for cancer.

Acknowledgments

Authors thank Hamdi Mango Center for Scientific Research and faculty of medicine at the University of Jordan for their collaboration in SEM, TEM and TGA measurements.

ORCID iDs

Mohyeddin Assali https://orcid.org/0000-0002-2286-9343

References

[1] Iijima S and Ichihashi T 1993 Single-shell carbon nanotubes of 1 nm diameter *Nature* **363** 603–5
[2] Baughman R H 2002 Carbon nanotubes—the route toward applications *Science* **297** 787–92
[3] Bianco A, Kostarelos K and Prato M 2005 Applications of carbon nanotubes in drug delivery *Curr. Opin. Chem. Biol.* **9** 674–9
[4] Zhao Y, Xing G and Chai Z 2008 Nanotoxicology: are carbon nanotubes safe? *Nat. Nanotechnol.* **3** 191–2
[5] Liu Z, Davis C, Cai W, He L, Chen X and Dai H 2008 Circulation and long-term fate of functionalized, biocompatible single-walled carbon nanotubes in mice probed by Raman spectroscopy *Proc. Natl Acad. Sci.* **105** 1410–5
[6] Guo J, Zhang X, Li Q and Li W 2007 Biodistribution of functionalized multiwall carbon nanotubes in mice *Nucl. Med. Biol.* **34** 579–83
[7] Matsumura Y and Maeda H 1986 A new concept for macromolecular therapeutics in cancer chemotherapy: mechanism of tumoritropic accumulation of proteins and the antitumor agent smancs *Cancer Res.* **46** 6387–92
[8] Boucher Y, Baxter L T and Jain R K 1990 Interstitial pressure gradients in tissue-isolated and subcutaneous tumors: implications for therapy *Cancer Res.* **50** 4478–84
[9] Pawar V K, Singh Y, Meher J G, Gupta S and Chourasia M K 2014 Engineered nanocrystal technology: *in vivo* fate, targeting and applications in drug delivery *J. Control. Release* **183** 51–66
[10] Dvorak H F, Nagy J A, Dvorak J and Dvorak A 1988 Identification and characterization of the blood vessels of solid tumors that are leaky to circulating macromolecules *Am. J. Pathol.* **133** 95–109
[11] Eberhard A, Kahlert S, Goede V, Hemmerlein B, Plate K H and Augustin H G 2000 Heterogeneity of angiogenesis and blood vessel maturation in human tumors: implications for antiangiogenic tumor therapies *Cancer Res.* **60** 1388–93

[12] McGown A T and Fox B W 1989 Structural and biochemical comparison of the anti-mitotic agents colchicine, combretastatin A4 and amphethinile *Anti-Cancer Drug Des.* **3** 249–54
[13] Tozer G M, Kanthou C, Parkins C S and Hill S A 2002 The biology of the combretastatins as tumour vascular targeting agents *Int. J. Exp. Pathol.* **83** 21–38
[14] Monk K A *et al* 2006 Design, synthesis, and biological evaluation of combretastatin nitrogen-containing derivatives as inhibitors of tubulin assembly and vascular disrupting agents *Bioorg. Med. Chem.* **14** 3231–44
[15] Bayless K J 2004 Microtubule depolymerization rapidly collapses capillary tube networks *in vitro* and angiogenic vessels *in vivo* through the small GTPase Rho *J. Biol. Chem.* **279** 11686–95
[16] Lin H L *et al* 2007 Combretastatin A4-induced differential cytotoxicity and reduced metastatic ability by inhibition of AKT function in human gastric cancer cells *J. Pharmacol. Exp. Ther.* **323** 365–73
[17] Shen C-H, Shee J-J, Wu J-Y, Lin Y-W, Wu J-D and Liu Y-W 2010 Combretastatin A-4 inhibits cell growth and metastasis in bladder cancer cells and retards tumour growth in a murine orthotopic bladder tumour model *Br. J. Pharmacol.* **160** 2008–27
[18] Zhang Y-f, Wang J-c, Bian D-y, Zhang X and Zhang Q 2010 Targeted delivery of RGD-modified liposomes encapsulating both combretastatin A-4 and doxorubicin for tumor therapy: *in vitro* and *in vivo* studies *Eur. J. Pharm. Biopharm.* **74** 467–73
[19] Nallamothu R *et al* 2006 A tumor vasculature targeted liposome delivery system for combretastatin A4: design, characterization, and *in vitro* evaluation *AAPS PharmSciTech* **7** E7–16
[20] Wang Z, Chui W-K and Ho P C 2010 Nanoparticulate delivery system targeted to tumor neovasculature for combined anticancer and antiangiogenesis therapy *Pharm. Res.* **28** 585–96
[21] Falciani C *et al* 2010 Design and *in vitro* evaluation of branched peptide conjugates: turning nonspecific cytotoxic drugs into tumor-selective agents *ChemMedChem* **5** 567–74
[22] Kolb H C, Finn M G and Sharpless K B 2001 Click chemistry: diverse chemical function from a few good reactions *Angew. Chem., Int. Ed. Engl.* **40** 2004–21
[23] Kolb H C and Sharpless K B 2003 The growing impact of click chemistry on drug discovery *Drug Discovery Today* **8** 1128–37
[24] Wang R *et al* 2007 SWCNT PEG-eggs: single-walled carbon nanotubes in biocompatible shell-crosslinked micelles *Carbon* **45** 2388–93
[25] Iverson N M *et al* 2013 *In vivo* biosensing via tissue-localizable near-infrared-fluorescent single-walled carbon nanotubes *Nat. Nanotechnol.* **8** 873–80
[26] Singh S *et al* 2012 Functionalized carbon nanotubes: biomedical applications *Int. J. Nanomed.* **7** 5361–74
[27] Assali M, Leal M P, Fernández I and Khiar N 2013 Synthesis and non-covalent functionalization of carbon nanotubes rings: new nanomaterials with lectin affinity *Nanotechnology* **24** 085604
[28] Xiao C-F, Zou Y, Du J-L, Sun H-Y and Liu X-K 2012 Hydroxyl substitutional effect on selective synthesis ofcis, transStilbenes and 3-Arylcoumarins through Perkin condensation *Synth. Commun.* **42** 1243–58
[29] Dulbecco R and Vogt M 1954 Plaque formation and isolation of pure lines with poliomyelitis viruses *J. Exp. Med.* **99** 167–82
[30] Green M R and Sambrook J 1989 *Molecular Cloning: A Laboratory Manual* 2nd edn (Cold Spring Harbor, NY: Cold Spring Harbor Laboratory)
[31] Yau H C, Bayazit M K, Steinke J H G and Shaffer M S P 2015 Sonochemical degradation of N-methylpyrrolidone and its influence on single walled carbon nanotube dispersion *Chem. Commun.* **51** 16621–4
[32] Vermes I, Haanen C, Steffens-Nakken H and Reutellingsperger C 1995 A novel assay for apoptosis flow cytometric detection of phosphatidylserine expression on early apoptotic cells using fluorescein labelled annexin V *J. Immunol. Methods* **184** 39–51
[33] Vermes I, Haanen C and Reutelingsperger C 2000 Flow cytometry of apoptotic cell death *J. Immunol. Methods* **243** 167–90
[34] Kanthou C *et al* 2004 The tubulin-binding agent combretastatin A-4-phosphate arrests endothelial cells in mitosis and induces mitotic cell death *Am. J. Pathol.* **165** 1401–11